ACTA
PROTOZOOLOGICA

Acta Protozool. (2016) 55: 7–18
www.ejournals.eu/Acta-Protozoologica
doi:10.4467/16890027AP.16.002.4043

Description of *Epistylis camprubii* n. sp., a Species Highly Tolerant to Ammonium and Nitrite

Oriol CANALS and Humbert SALVADÓ

Laboratory of Protistology, Departament de Biologia Animal, Facultat de Biologia, Universitat de Barcelona, Barcelona, Spain

Abstract. A new peritrich species highly tolerant to ammonium and nitrite, *Epistylis camprubii* n. sp., was found adhered to the biofilm of two advanced wastewater treatment plants treating high ammonium-loaded wastewater in Rubí, Spain. Its morphology, oral infraciliature and phylogenetic position in the peritrich clade were studied. The new species is a vase-shaped peritrich, constricted below the peristomial lip, with an *in vivo* average length of 58.7 ± 10.1 μm, average width of 32.0 ± 5.4 μm, and a longitudinally striated, compact stalk that occasionally exhibits uneven thickness and rarely shows transverse segments. The peristomial disc is commonly rounded or pointed, and rarely umbilicated. The C-shaped macronucleus is located in the adoral half of the body, and the only contractile vacuole lies in the adoral third of the zooid. The molecular analysis of the 18s gene sequence clustered *E. camprubii* n. sp. together with the other *Epistylis*, with the exception of *Epistylis galea*.

Key words: Peritrichia, wastewater treatment, ciliates, 18s rRNA, ammonium, nitrite.

Abbreviations: A/O SBNR – Anoxic/Oxic Shortcut Biological Nitrogen Removal; PN – Partial Nitrification; MBBR – Moving Bed Biofilm Reactor.

INTRODUCTION

The genus *Epistylis* Ehrenberg, 1830 comprises a great number of species from aquatic environments including both freshwater and marine ecosystems. The *Epistylis* species are colonial and normally attached to a non-living substrate, although several species are known to be capable of living as epibiont on aquatic invertebrates (Stiller 1971). Just a few species have been described as free-living. *Epistylis* zooids are usually elongated, showing one micronucleus and a macronucleus, an eversible peristomial lip, and a non-contractile stalk without a spasmoneme. *Epistylis* are very common in wastewater treatment systems, and play an important role in effluent clarification. In addition, *Epistylis* species of wastewater treatment plants can be used as performance bioindicators of a great variety of parameters and processes (Curds 1982, Salvadó *et al*. 1995, Berger and Foissner 2003, Canals *et al*. 2013).

Address for correspondence: Oriol Canals and Humbert Salvadó, Laboratory of Protistology, Departament de Biologia Animal, Facultat de Biologia, Universitat de Barcelona. Avinguda Diagonal 643, 08028 Barcelona, Spain. Telephone number: +34 93 4021440; Fax number: +34 93 403 5740; E-mail: ocanalsd@gmail.com; hsalvado@ub.edu.

Epistylis camprubii n. sp. was found and collected from two advanced treatment plants treating high ammonium wastewater. Firstly identified as *Epistylis* cf. *rotans*, a deeper study provided enough evidences to consider this organism, which is highly tolerant to ammonium and nitrite, as a new *Epistylis* species. It was named *Epistylis camprubii* n. sp. The present study describes the morphologic and molecular characteristics of the new *Epistylis* species, and provides detailed images and drawings of its oral infraciliature.

MATERIAL AND METHODS

1. Sampling. Samples containing *Epistylis camprubii* n. sp. were obtained by analysing the microfauna of an *Anoxic/Oxic Shortcut Biological Nitrogen Removal Moving Bed Biofilm Reactor* (A/O SBNR-MBBR) and a *Partial Nitritation Moving Bed Biofilm Reactor* (PN-MBBR). Both pilot wastewater treatment plants were located in Rubí, Spain, and operated during different periods. A *Moving Bed Biofilm Reactor* (MBBR) process is characterised by the presence of plastic supports held in suspension (named 'carriers'), on which the biofilm develops. *Epistylis camprubii* n. sp. was mainly observed attached to the biofilm of carriers. Consequently, the biofilm needed to be detached from the carriers to undertake the study. The method of detachment is detailed in Canals *et al*. (2013).

2. Morphological analysis. The length and width of the zooid, the peristomial disc diameter, the height and width of peristomal lip, and the stalk width (see Fig. 1d) were measured using a Zeiss Axioskop 40 microscope. Measurements were always made on *in vivo* specimens, using a calibrated ocular micrometer. The ammoniacal silver carbonate method (Fernández-Galiano 1994) was carried out to study the oral infraciliature of the stained specimens. Ammoniacal silver carbonate and Klein's silver impregation (Klein 1958) methods were used to determine the number of transverse silverlines of the stained zooids. Pictures were taken on a ProgResC3 camera (Jenoptik, Germany) and Zeiss Axioskop 40 and Leitz DMRB microscopes for *in vivo* and stained specimens respectively. Drawings were made using Illustrator software based on *in vivo* and after silver staining method specimens.

3. Single Cell PCR, sequencing and data analysis. Isolated cells of *Epistylis camprubii* n. sp. were collected in a 0.2-mL PCR tube and frozen at –80°C until PCR was performed. The cells were isolated using an inverted microscope (Meiji TC5000). To perform Single Cell amplifications, the following primer combinations were used: 528F (5'-GCGGTAATTCCAGCTCCAA-3', Elwood *et al*. 1985) and EukR (5'-TGATCCTTCTGCAGGTTCACCTAC-3', EUK B, Medlin *et al*. 1988). The PCR mixtures (100 µL of volume) contained: 20 µL approximately of the culture medium from which each cell (DNA template) was isolated, 2 µL of deoxynucleoside triphosphate mix at a concentration of 10 mM each, 4 µL of $MgCl_2$ (50 mM solution), 10 µL of PCR buffer (Invitrogen; USA), 8 µL of each primer at a concentration of 10 µM, 0.75 µL of Taq DNA polymerase (Invitrogen) and 47.25 µL of 0.2 µm-filtered sterilised water (up to 100 µL). The PCR program included an initial denaturation at 94°C for 5 min, followed by 30 cycles of denaturation at 94°C for 1 min, annealing at 56°C for 1 min, extension at 72°C for 3 min, and a final extension cycle at 72°C for 10 min. An aliquot of the PCR product was run in a 1% agarose gel by electrophoresis, stained with SYBR SAFE (0.5 × final concentration; Invitrogen), and checked by comparison to a standard (Low DNA Mass Ladder; Invitrogen).

PCR products were sent to Genoscreen (Lille, France) to be purified and subsequently sequenced with the primers 528F, EukR (both sequences detailed previously), 1209F (5'-CAGGTCTGTGATGCCC-3', Littlewood and Olson 2001) and 1209R (5'-GGGCATCACAGACCTG-3', Giovannoni *et al*. 1988). The sequences obtained for each sample were assembled using Geneious software and the resulting consensus sequence was screened and then compared with public DNA databases using BLAST (Altschul *et al*. 1997). The sequence can be found in GenBank (accession number KP713786).

To study the phylogenetic position of *Epistylis cambrubii* n. sp. in the Peritrichia phylogenetic tree, as well as its position within the *Epistylis* clade, some previously published sequences from GenBank were used in addition to the sequence obtained for *E. camprubii*: *Campanella umbellaria* AF401524; *Carchesium polypinum* GU187053; *Cyclidium glaucoma* EU032356; *Epicarchesium abrae* DQ190462; *Epistylis chlorelligerum* KM096375; *Epistylis chrysemydis* AF335514; *Epistylis galea* AF401527; *Epistylis hentscheli* AF335513; *Epistylis plicatilis* AF335517; *Epistylis riograndensis* KM594566; *Epistylis urceolata* AF335516; *Epistylis wenrichi* AF335515; *Opercularia microdiscum* AF401525; *Pseudovorticella punctata* DQ190466; *Pseudovorticella sinensis* DQ845295; *Tetrahymena pyriformis* EF070255; *Vaginicola crystallina* AF401521; *Vorticella aequilata* JN120215; *Vorticella convallaria* JN120220; *Vorticellides aquadulcis* JQ723990; *Vorticellides infusionum* JN120203; *Vorticellides microstoma* JN120206; *Zoothamnium alternans* DQ662855 and *Zoothamnium pluma* DQ662854.

The 18s rRNA sequences were aligned with MAFFT V.6 online software (Katoh and Toh 2008), using the Q-INS-i approach with default settings (gap opening penalty GOP = 1.53 and offset value set to 0.0). Gaps were recoded as presence/absence data following the simple method of Simmons and Ochotorena (2000), as implemented in the program SeqState v1.4.1 (Müller 2005). The final matrix had 1819 nucleotide position and 90 characters corresponding to the gaps scored as absence/presence. The best-fitting evolutionary model of the alignment was assessed using Partitionfinder software (Lanfear *et al*. 2012). The suggested model (GTR+G+I) was used for subsequent analysis.

Phylogenetic trees were inferred using three methods: maximum parsimony (MP), maximum likelihood (ML) and Bayesian inference (BI). MP analysis was carried out using TNT software (Goloboff *et al*. 2008) with gaps scored as absence/presence. The search consisted of 1000 replicates of random sequence addition, followed by TBR branch swapping and holding five trees per iteration. Clade support was assessed with 1000 bootstrap replicates. Maximum likelihood inference was conducted using RAxML v.8.1.16 program (Stamatakis 2014) run under the RAxML-GUI software (Silvestro and Michalak 2012). Two independent models were defined, a GRT+G+I for the nucleotide and a binary model for the gap partition. The best tree was selected from 100 iterations and support assessed with 1000 replicates of bootstrap resampling. Bayesian Inference was conducted using MrBayes 3.2 (Ronquist and Huelsenbeck 2003). Two independent runs of 5×10^7 genera-

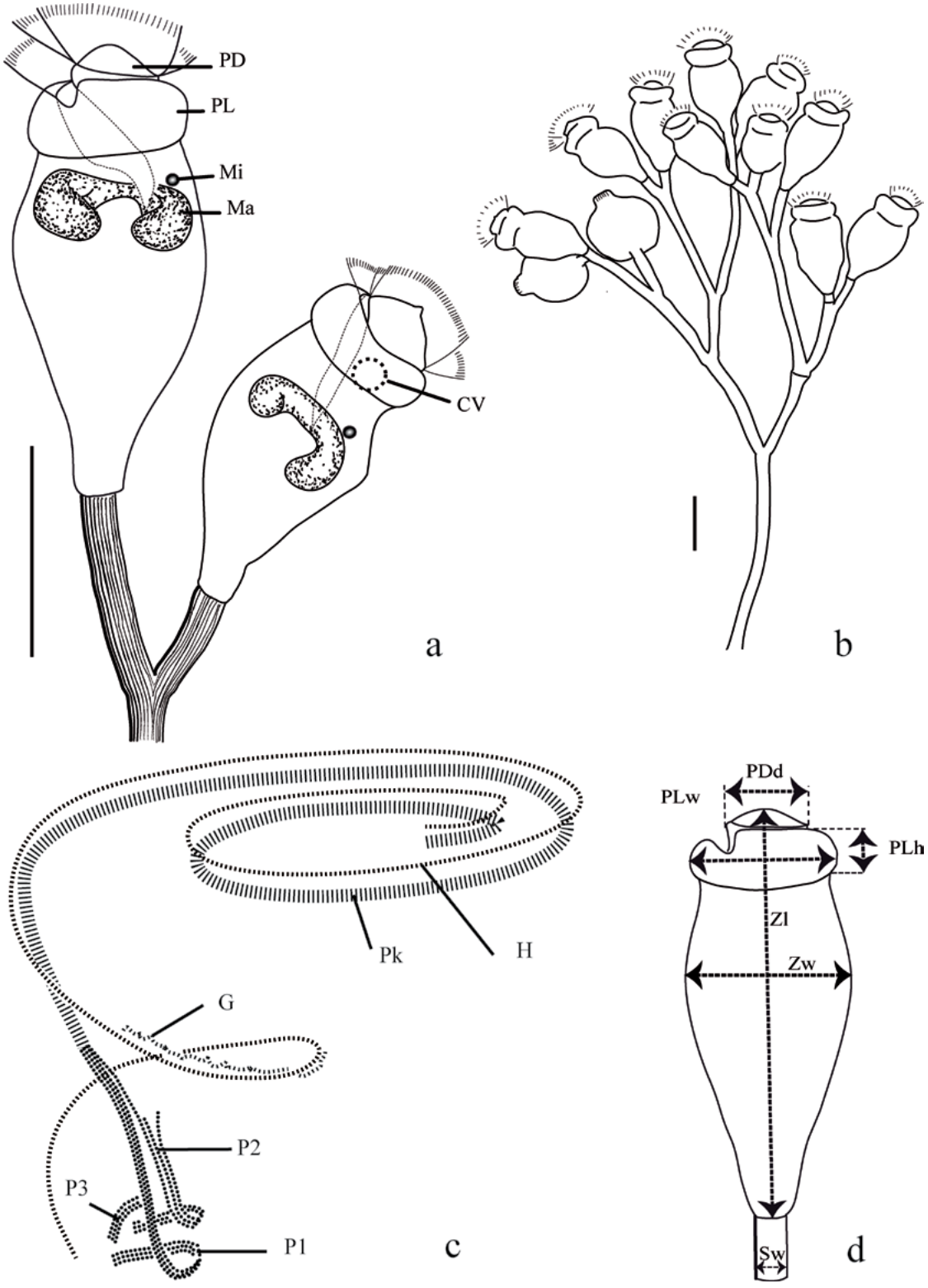

Fig. 1a–d. Morphological and oral infraciliature details of *Epistylis camprubii*. **a** – detail of the zooid. PD – peristomial disk; PL – peristomial lip; CV – contractile vacuole; Ma – macronucleus; Mi – micronucleus; **b** – scheme of a colony; **c** – oral infraciliature. Pk – polykinety; H – haplokinety; G – germinal kinety; P1 – polykinety 1; P2 – polykinety 2; P3 – polykinety 3; **d** – morphological characteristics measured. PDd – peristomial disk diameter; PLw – peristomial lip width; PLh – peristomial lip height; Zl – zooid lenght; Zw – zooid width; Sw – stalk width. Scale bars: 25 μm.

tions with 4 MCMC (Markov Chain Monte Carlo) chains per run, starting from random trees and resampling each 1000 generations were run simultaneously. The first 25% generations of each run were discarded as a burn-in for the analyses. Run convergence was assessed by means of the average standard deviation of split frequencies (ASDSF < 0.01).

RESULTS

Epistylis camprubii n. sp.

1. Diagnosis. Freshwater bacterivorous *Epistylis*, measuring on average 58.7 µm in length and 32.0 µm in width. The zooids are vase-shaped and constricted below the thick peristomial lip. Persitomial disc commonly rounded or pointed, very rarely umbilicated. C-shaped macronucleus located in the adoral half of the zooid and transversely oriented. Contractile vacuole placed in the adoral third of the body, on dorsal wall of infundibulum. Row 3 of P2 slightly divergent to the other rows at their abstomal ends, extending, together with row 2, approximately 2/3 of the length of row 1. Transverse silverlines numbering 106 to 136 from peristome to aboral trochal band and 33 to 48 from aboral trochal band to scopula.

2. Description. *Epistylis camprubii* n. sp. is a vase-shaped peritrich, constricted below the peristomial lip. The zooid length ranges from 35.3 to 98.1 µm (average of 58.7 ± 10.1 µm) and the width from 18.0 to 65.2 µm (average of 32.0 ± 5.4 µm). The peristomial disc is commonly rounded or pointed, and very rarely umbilicated. It is possible, but not common, to observe zooids of the same colony showing different peristomial disc shapes. The diameter of the peristomial disc ranges from 11.2 to 21.3 µm (average of 15.5 ± 1.9 µm). *E. camprubii* shows a thick peristomial lip with a height ranging from 5.0 to 10.6 µm (average of 7.8 ± 1.2 µm) and a width from 16.2 to 31.7 µm (average of 24.2 ± 2.9 µm). The width of the stalk varies from 3.1 to 8.4 µm (average of 5.3 ± 0.9 µm). The stalk is longitudinally striated and compact, occasionally exhibits uneven thickness, and rarely shows transverse segments. Stalk thickening is often associated with separation nodes, but they can also be seen in the internodal part of the stalk (Fig. 2h–j). Thicker stalks or branches, as well as more frequent stalk thickening, are related to shorter stalks. *E. camprubii* presents a colourless cytoplasm and a transversely oriented C-shaped macronucleus located in the adoral half of the zooid. The only contractile vacuole lies in the adoral third of the body, on dorsal wall of infundibulum.

In the wastewater treatment systems where *E. camprubii* was found, 88.2% of the colonies showed a number of zooids between 2 and 20 (Fig. 4), with a maximum value of 124. The ramification is initially dichotomic, but becomes irregular after the second level of ramification. Sometimes the ramification is totally irregular.

E. camprubii presents the typical oral infraciliature of the genus *Epistylis*. Specifically, it has very similar oral infraciliature to *Epistylis chrysemydis* (detailed by Foissner *et al*. 1992). The haplokinety and the polykinety make between one and one and a half circuits before entering the infundibulum, where they make a turn again. In the infundibulum, the haplokinety is initially accompanied by a germinal kinety. The germinal kinety is no longer observed when the haplokinety turns and follows the longitudinal axis of the zooid. The polykinety becomes three infundibular polykineties (named P1, P2, P3), each consisting of 3 rows of kinetosomes. The abstomal end of P1 comes directly from the original polykinety and its three rows are equal in length. The abstomal end of row 1 of P2 extends the entire distance to P1 and merges with it near the oral opening. Rows 2 and 3 of P2 are much shorter than row 1, extending only ~ 2/3 of the length of row 1 at their abstomal ends. Row 3 of P2 is slightly divergent from the other two rows at its abstomal end. The adstomal ends of all three rows of P2 end a short distance before the adstomal ends of P1 and P3. P3 is the shortest polykinety and presents the three rows equal in length. P3 appears after the last turn of P1 and P2 and its adstomal end is very close to the adstomal end of P1 (Figs 1c and 3d–e).

Epistylis camprubii presents 106 to 136 transverse silverlines from peristome to aboral trochal band and 33 to 48 from aboral trochal band to the scopula.

3. Etymology. The name *camprubii* refers to the surname of the Catalan biologist Jordi Camprubí Capella, in personal recognition of a life dedicated to teaching and sharing his love for biology, especially for ciliate protozoa.

▸▸

Fig. 2a–j. Images of *Epistylis camprubii, in vivo*. **a–b –** example of colonies; **c–d** – two examples of extended zooids; **e** – zooid during conjugation; **f** – conjugation; **g** – contracted zooid; **h–j** – images of the stalk and branches, from smoother and larger to shorter and thicker. Scale bars: 25 µm.

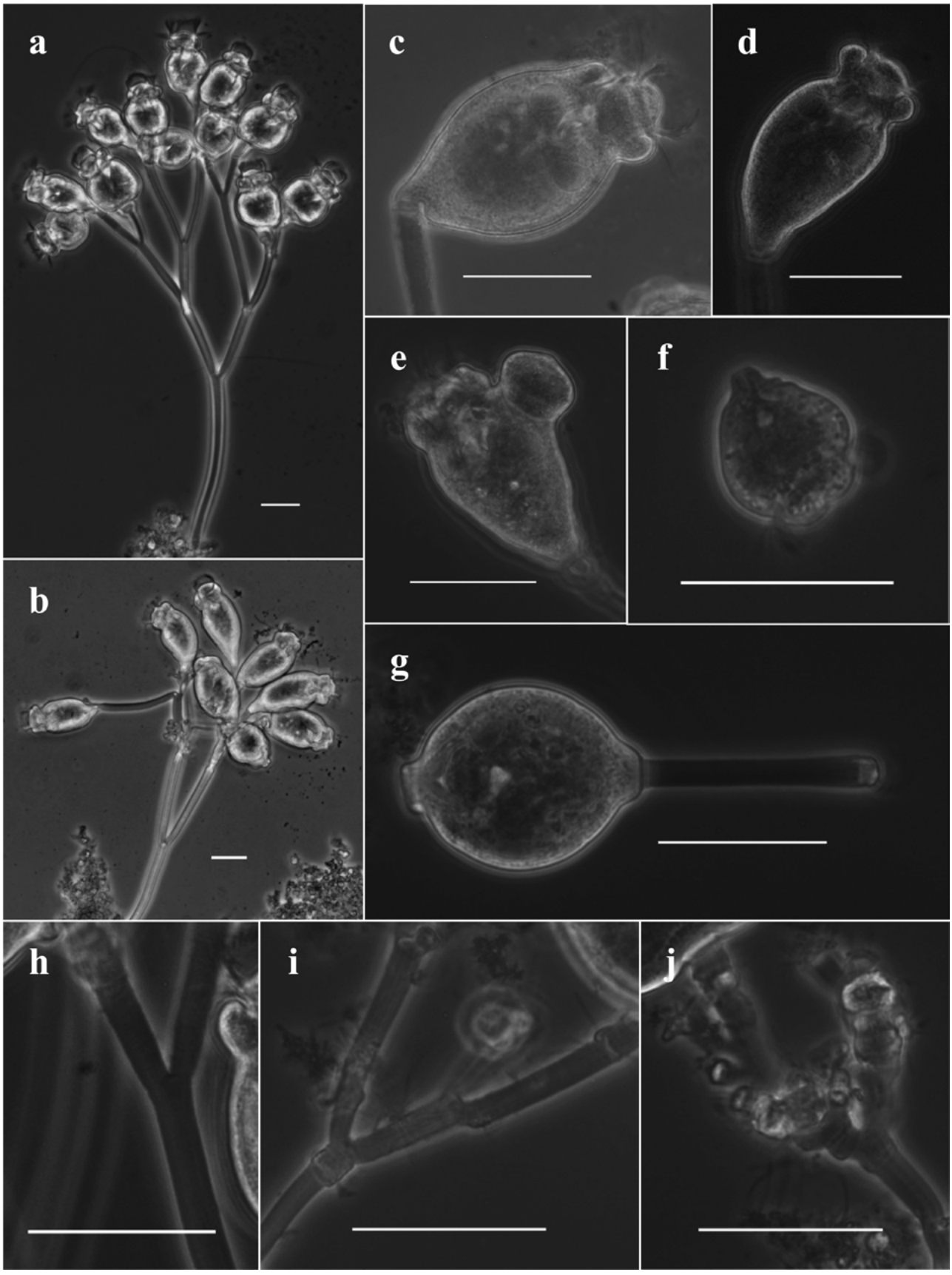
a
c
d
e
f
b
g
h
i
j

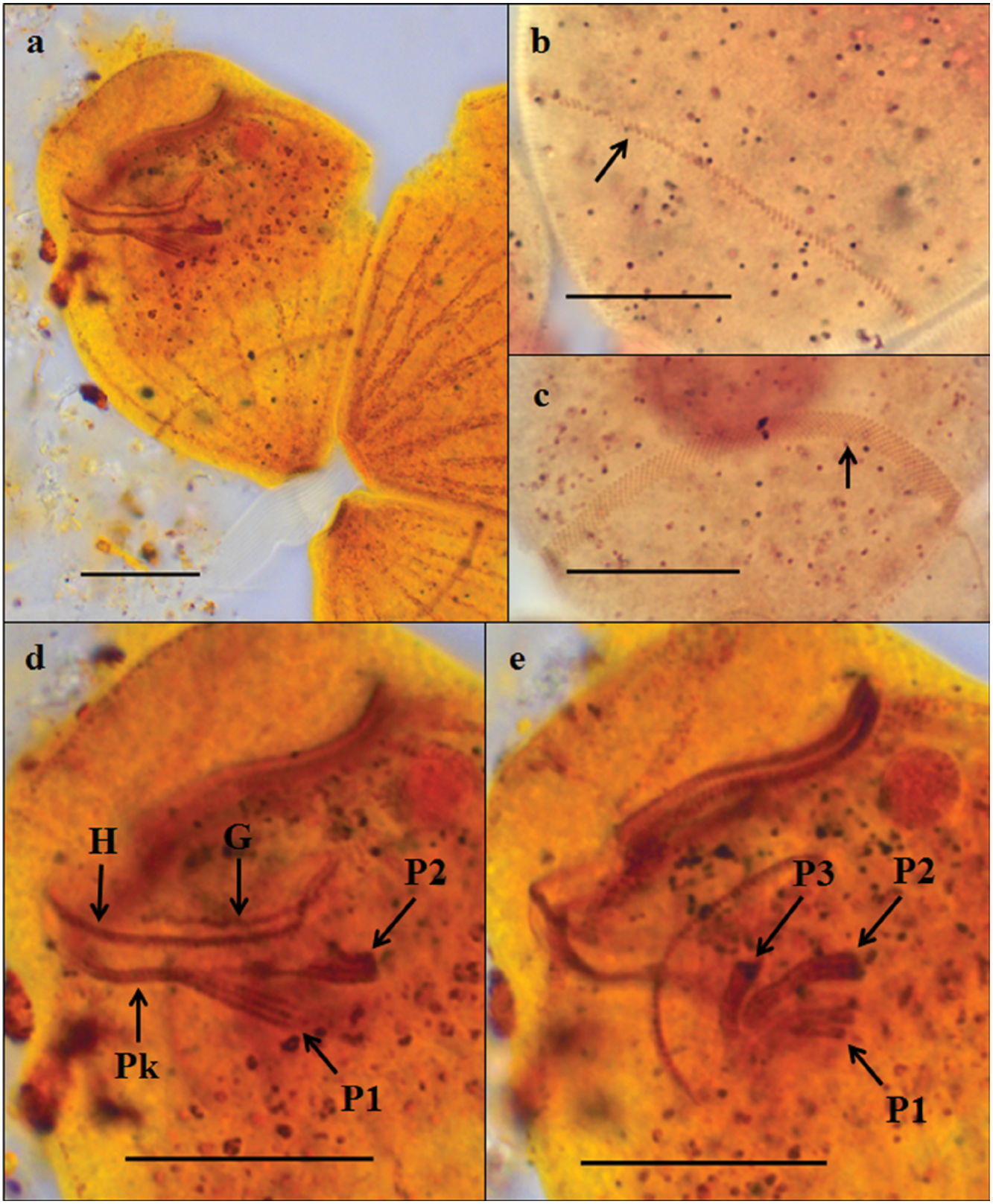

Fig. 3a–e. Images of *Epistylis camprubii*, after silver staining method. **a** – view of the longitudinal fibers and the oral infraciliature; **b** – detail of the aboral trochal band of a feeding zooid; **c** – aboral trochal band of a zooid during swimmer formation; **d–e** – oral infraciliature details. H – haplokinety; G – germinal kinety; Pk – polykinety; P1 – polykinety 1; P2 – polykinety 2; P3 – polykinety 3. Scale bars: 15 µm.

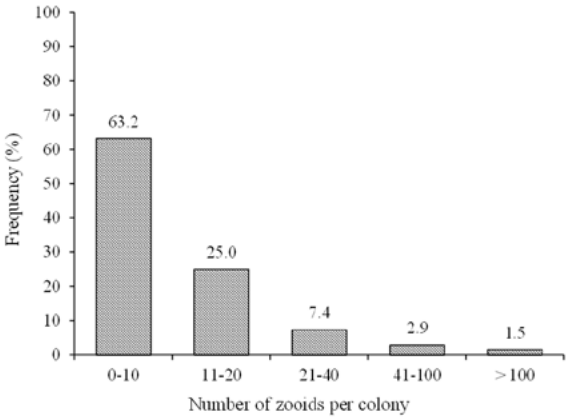

Fig. 4. Frequency of the number of zooids per colony observed in *Epistylis camprubii* colonies (number of analyzed colonies = 71).

4. Ecology. *Epistylis camprubii* is a bacterivorous peritrich. It was first observed in the aerobic reactor of an A/O SBNR-MBBR process and was initially identified as *Epistylis* cf. *rotans* (Canals *et al*. 2013). It was observed mainly inhabiting the biofilm adhered to carriers (the plastic support for the biofilm attachment), but was also found colonising the liquid phase, adhered to flocs. It was observed again attached to the biofilm and colonising the liquid phase of a PN-MBBR and PN-granular processes, both previous to an Anammox reactor.

A/O SBNR and PN processes are designed to treat high ammonium-loaded wastewater (up to over 10^3 $N\text{-}NH_4^+$ $mg \cdot L^{-1}$). Specifically, the aerobic reactor of an A/O SBNR process is designed to oxidise the ammonium in the influent and accumulate the oxidised nitrogen form as nitrite, while the PN process is focused on achieving an adequate effluent for the posterior Anammox reactor, that is, a nitrite: ammonium ratio close to 1.2. The range of ammonium and nitrite values in which *Epistylis camprubii* was observed are shown in Table 2.

Some organisms were identified cohabiting with *E. camprubii*: the ciliates *Colpoda* spp., *Cyclidium glaucoma*, *Opercularia coarctata*, *Telotrochidium matiense*, *Vorticellides microstoma*-complex and two unidentified Hypotrichia; *Tetramitus rostratus*, *Polytoma* sp., *Anthophysa* sp. and *Trimastix* sp. among other unidentified flagellates; nematoda; and unidentified gymnamoeba smaller than 20 μm. Most of these species, specifically the ciliates, are usually observed in conventional activated sludge wastewater treatment plants. It would not be surprising if *Epistylis camprubii* had been misidentified in this kind of treatment systems.

5. Type Sequence. GenBank accession number KP713786.

6. Type material. An holotype slide with 36 specimens (registration number CRBA-28006) and a paratype slide with 52 specimens (registration number CRBA-28007) after ammoniacal silver carbonate method were deposited in the Centre de Recursos de Biodiversitat Animal (CRBA), Facultat de Biologia, Universitat de Barcelona, Barcelona (Spain). Another paratype slide with 35 specimens was deposited in the Natural History Museum of London, UK (registration number NHMUK 2015.4.20.1).

7. Phylogenetic position. The molecular analysis of the 18s rRNA gene sequences supported the inclusion of *E. camprubii* within the Peritrichia, regardless of the inference method implemented. All analyses agreed in supporting the monophyly of *E. camprubii* with the other *Epistylis* sequences used in the present study, with the single exception of *E. galea* (Fig. 5).

8. Comparative diagnosis. A large number of *Epistylis* species have been described. Among them, just a few showed morphological similarities to *E. camprubii* and/or are typical species of wastewater treatment plants.

E. camprubii was formerly reported as *Epistylis* cf. *rotans* (Canals *et al*. 2013), since *E. rotans* is a vase-shaped peritrich that is often observed in wastewater treatment plants, and presents a longitudinally striated and transversally segmented stalk, as *E. camprubii* does. But further observations revealed that transverse segments are not always present in *E. camprubii*, in contrast to *E. rotans*. Moreover, *E. rotans* is longer (70 to 100 μm) and was described as an oligosaprobic species by Curds (1969), while *E. camprubii* is shorter (Table 1), inhabits more polluted environments, and shows a high tolerance to ammonium and nitrite compounds (Table 2). It must be noted that Foissner *et al*. (1992) considers *E. rotans* a synonym of *E. procumbens*, a funnel-shaped peritrich with a zooid length from 60 to 140 μm, often bent and with transverse segments before the stalk division, whose characteristics clearly do not match those of *E. camprubii*.

A comparison of *E. camprubii* and other *Epistylis* species of wastewater treatment plants showed that *E. camprubii* is shorter than *E. chrysemydis* (120 to 220 μm), *E. coronata* (70 to 120 μm), *E. entzii* (125 to 190 μm), *E. hentscheli* (110 to 170 μm), *E. balatonica* (90 to 100 μm) and *E. plicatilis* (90 to 160 μm). In addition, most of these species have a wider stalk, ranging from 7 to 20 μm width (Foissner *et al*. 1992), while the stalk of *E. camprubii* ranges from 3.1 to a maxi-

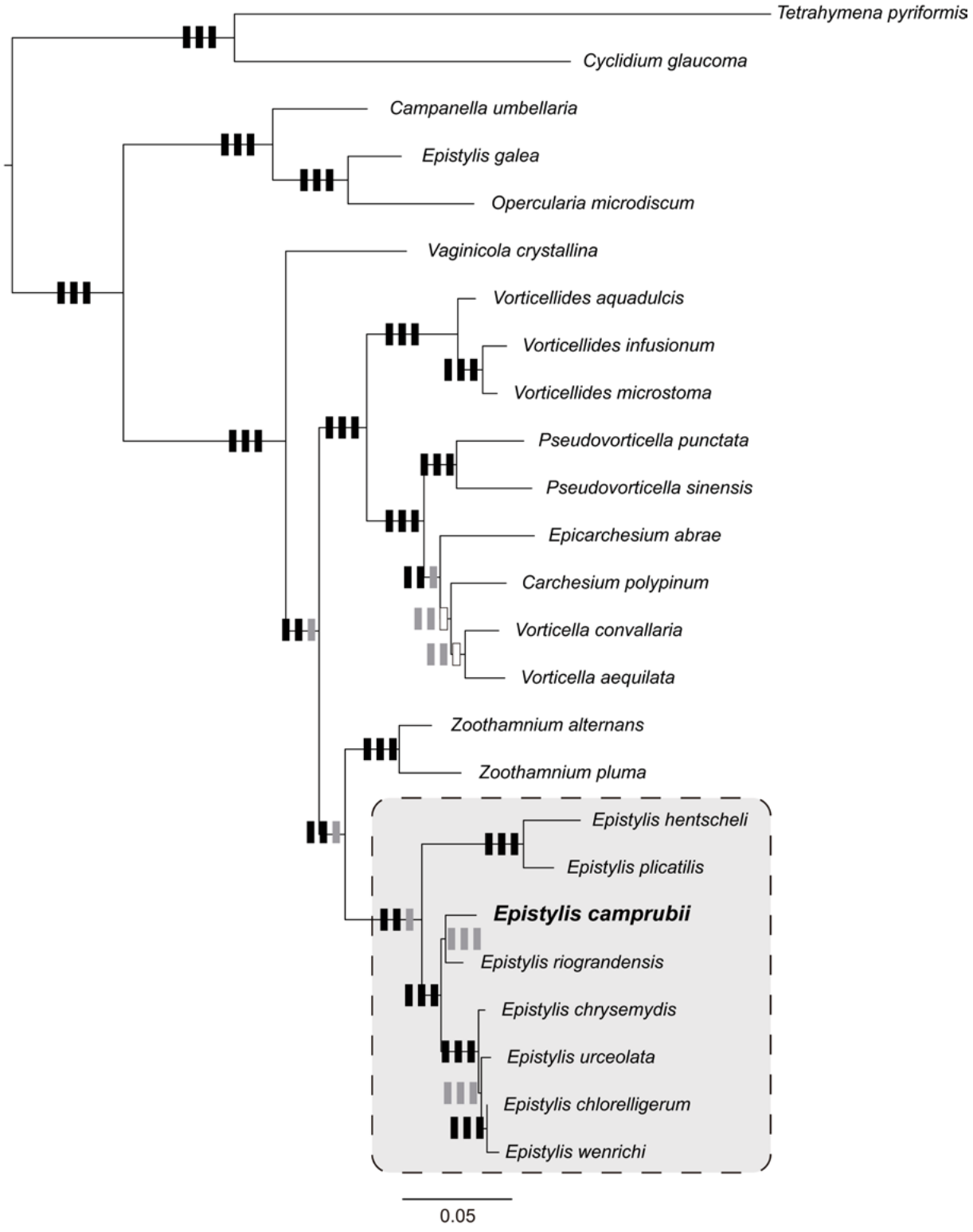

Fig. 5. The preferred 18s rRNA tree under maximum likelihood (ML). Rectangles on branches denote the support recovered in analyses under alternative inference methods. Left rectangle refers to maximum likelihood (ML), the middle one to Bayesian inference (BI) and the right one to maximum parsimony (MP). Black coloured rectangle indicates bootstrap support > 80 or posterior probability > 0.95, grey rectangle indicates clade recovered but with lower support than the former values, and white rectangle indicates the clade was not recovered. Main *Epistylis* clade boxed.

mum of 8.4 µm when stalk thickening occurs (Table 1). Other clearly different traits are that *E. chrysemydis* and *E. balatonica* have two lips in the peristome, in contrast to the one lip of *E. camprubii*. *E. coronata* always shows an umbilicated peristomial disc and *E. plicatilis* and *E. hentscheli* are clearly funnel-shaped.

Outside the field of wastewater treatment systems, three *Epistylis* species presented similar characteristics to *E. camprubii*: *E. epistyliformis*, *E. thienemanni* and *E. variabilis* (Stiller 1971). *E. epistyliformis*, the most similar species, is a vase-shaped peritrich with a clearly pointed and rarely umbilicated peristomial disc, a zooid length from 43 to 62 µm, and clearly constricted below the peristomial lip. Nevertheless, the C-shaped macronucleus of *E. epistyliformis* is flattened, located in half of the body, and follows the longitudinal axis of the zooid, in contrast to the transverse position of the macronucleus of *E. camprubii*. In addition, Stiller's guide (1971) does not specify in the text or in the drawings whether the stalk of *E. epistyliformis* is longitudinally striated or not. *E. variabilis* shows variability in the stalk and branches that strongly resembles that of *E. camprubii*. Colonies of *E. variabilis* inhabiting calm waters present long and smooth branches, while the branches of colonies from vigorous water flows are shorter, articulated and thicker or show uneven thickness. Nevertheless, there is no information on the specific width of the stalk in *E. variabilis*, and the main stalk of the colony is always short, a feature that does not always occur in *E. camprubii*. Moreover, *E. variabilis* zooids are funnel-shaped, in contrast to the vase-shaped zooids of *E. camprubii*. Finally, *E. thienemanni*

Table 1. Mean, standard deviation (SD), maximum values (Max), minimum values (Min), coefficient of variation (CV) and number of measurements realized (N) of morphological characteristics of *Epistylis camprubii*.

	Mean	SD	Max	Min	CV	N
Zooid length, *in vivo* (µm)	58.7	10.1	98.1	35.3	17.2	343
Zooid width, *in vivo* (µm)	32.0	5.4	65.2	18.0	16.8	342
Peristomial disc diameter, *in vivo* (µm)	15.5	1.9	21.3	11.2	12.1	94
Peristomial lip height, *in vivo* (µm)	7.8	1.2	10.6	5.0	15.9	149
Peristomial lip width, *in vivo* (µm)	24.2	2.9	31.7	16.2	11.8	110
Stalk width, *in vivo* (µm)	5.3	0.9	8.4	3.1	16.9	152
Number of silverlines from peristome to aboral trochal band	120.8	10.1	136.0	106.0	8.4	11
Number of silverlines from aboral trochal band to scopula	40.7	5.1	48.0	33.0	12.5	11
Macronucleous characteristics	C-shaped, transversely oriented, in the adoral half of the cell					
Number of contractile vacuoles, position	One, in the adoral third of the body, on dorsal wall of vestibulum					

Table 2. Minimum (Min) and maximum values (Max) of the main physicochemical parameters in which *Epistylis camprubii* was observed, and comparison with available ecological data of other *Epistylis* species.

	Epistylis camprubii	*E. chrysemydis*	*E. coronata*	*E. hentscheli*	*E. plicatilis*	*E. rotans/ E. procumbens*
	Min–Max	Min–Max	Min–Max	Min–Max	Min–Max	Min–Max
Soluble Chemical Oxygen Demand ($mg \cdot L^{-1}$)	53.8–415.3	–	–	–	–	–
Ammonium ($N\text{-}NH_4^+$, $mg \cdot L^{-1}$)	0.54–491	2.1–5.9	0–1.6	0–1.9	0–27	0–0.018
Free ammonia ($N\text{-}NH_3$, $mg \cdot L^{-1}$)	0.024–18.01	–	–	–	–	–
Nitrites ($N\text{-}NO_2^-$, $mg \cdot L^{-1}$)	0–572.1	0.1–0.8	–	–	0–61	–
Free nitrous acid ($N\text{-}HNO_2$, $mg \cdot L^{-1}$)	0.00013–0.47	–	–	–	–	–
Nitrates ($N\text{-}NO_3^-$, $mg \cdot L^{-1}$)	0–321	1.5–4.2	–	–	0.14–52	–
Temperature (°C)	22.6–33.6	10–35	2–12	2–32	6.6–32	6–23
pH	6.3–8.66	7.0–8.6	7.2–7.6	7.0–8.6	4.7–8.5	7.2–7.8

Table 3a. Comparison between *Epistylis camprubii* and the other *Epistylis* species mentioned in the manuscript: characteristics of zooid and persitome.

Species	Body lenght *in vivo* (µm)	Body width *in vivo* (µm)	Zooid shape	Peristomial disc diameter *in vivo* (µm)	Peristomial disc shape	Peristomial lip height *in vivo* (µm)	Peristomial lip width *in vivo* (µm)	Number of peristomial lips	Data source
Epistylis camprubii	35.3–98.1	18.0–65.2	Vase-shaped	11.2–21.3	Rounded, pointed, rarely umbilicated	5.0–10.6	16.2–31.7	1	Present manuscript
E. balatonica	90–100	45–55	Vase-shaped	–	–	–	–	2	Stiller 1971
E. chrysemydis	120–220	60–110	Vase-shaped	–	Umbilicated	–	50–80	2	Foissner *et al*. 1992
E. coronata	70–120	–	Vase-shaped	–	Slightly umbilicated and oblique	–	32–65	1	Foissner *et al*. 1992
E. entzii	125–190	80	Cylindrical	–	Convex, slightly oblique	–	–	1	Foissner *et al*. 1992
E. epistyliformis	43–62	20–27	Vase-shaped	–	Convex, sometimes conical	–	–	1	Stiller 1971
E. hentscheli	110–170	38–60	Asymmetric and bell-shaped, narrowed down to the stem	–	Convex, slightly oblique	–	–	1	Foissner *et al*. 1992
E. plicatilis	90–160	25–50	Funnel-shaped	–	Not umbilicated	–	36–60	1	Foissner *et al*. 1992
E. rotans/E. procumbens	60–140	2–2½ times as long as wide	Irregular (sigmoidal shape, bent at right angles, slightly tilted backwards)	–	Flat or slightly convex, slightly oblique	–	–	1	Foissner *et al*. 1999
E. rotans	70–100	–	Vase-shaped	–	Arched	–	–	1	Curds 1969
E. thienemanni	67–120	–	Vase-shaped	–	Conical	–	–	1	Stiller 1971
E. variabilis	50–100	–	Funnel-shaped	–	Slightly convex and obliquely protuberant	–	–	1	Stiller 1971

Table 3b. Comparison between *Epistylis camprubii* and the other *Epistylis* species mentioned in the manuscript: characteristics of stalk, macronucleus and contractile vacuole.

Species	Stalk width *in vivo* (µm)	Stalk striation / segmentation	Macronucleus	Contractile vacuole	Data source
Epistylis camprubii	3.1–8.4	Longitudinally striated, occasionally transeverse segmentation	C-shaped, transversely oriented; adoral half of the body	1, adoral third of the body, on dorsal wall of vestibulum	Present manuscript
E. balatonica	–	Longitudinally finely striated	Horinzotal horsehoe-shaped in the middle of the body	1, in the heigh of the peristomial lip	Stiller 1971
E. chrysemydis	13–25	Longitudinally striated, occasionally transeverse segmentation	C-shaped, transversely oriented; adoral half of the body	1, close or in the heigh of the peristomial lips, on ventral wall of vestibulum	Foissner *et al*. 1992
E. coronata	11–18	–	Semicircular, adoral half of the body	1, in the height of the peristomial lips, on dorsal wall of vestibulum	Foissner *et al*. 1992
E. entzii	18	–	3/4 circular, adoral half of the body	1, in the heigh of the peristomial lip, on dorsal wall of vestibulum	Foissner *et al*. 1992
E. epistyliformis	–	Transverse segmentation	Intenselly flattened, horsehoe-shaped	1, adoral third of the body	Stiller 1971
E. hentscheli	12–20, sometimes 25	Occasionally finely annulated	Semicircular, adoral half of the body	1, in the heigh of the peristomial lip, on ventral wall of vestibulum	Foissner *et al*. 1992
E. plicatilis	7–18	Longitudinally finely striated	Semicircular, adoral half of the body	1, in the heigh of the peristomial lip, on dorsal wall of vestibulum	Foissner *et al*. 1992
E. rotans/E. procumbens	–	Fine longitudinally striated, transverse segmentation	Reniform to semicircular, in transverse axis and adoral half of zooid	1, at level of peristomial lip, on dorsal wall of vestibulum	Foissner *et al*. 1999
E. rotans	–	Longitudinally striated, transeverse segmentation	C-shaped, transversely oriented, adoral third of the body	1, located in the adoral third of the body	Curds 1969
E. thienemanni	–	–	Flattened ribbon-like and horsehoe-shaped, adoral third of the body	1, located in the peristomial disc, on dorsal wall of vestibulum	Stiller 1971
E. variabilis	Variable	–	–	1, at the level of the peristomial lip	Stiller 1971

(Stiller 1971, first reported as *Rhabdostyla thienemanni* by Nenninger 1948) is an epibiont of leeches, and is larger (67 to 120 µm), but with a shorter stalk than *E. camprubii*. It has the contractile vacuole located in the peristomial disc. A summary of the comparison between *Epistylis camprubii* and the other *Epistylis* species can be seen in Tables 3a and 3b.

9. Comments. The great variability observed in the appearance of the stalk of *Epistylis camprubii* could be related to water hydrodynamics, as Stiller (1971) suggested regarding the stalk variability of *E. variabilis*. The authors also consider that the low number of zooids observed per colony (63% of colonies showed between 2 and 10 zooids, Fig. 4) may also be influenced or limited by the flow, agitation speed or other hydrodynamic parameters of water, in addition to the availability of food (bacteria) in the reactor. Further research is needed in order to shed light on these unanswered questions.

Acknowledgments. Thanks to Dr. Ramon Massana and Vanessa Balagué from Institut de Ciències del Mar (Barcelona, Spain) for their help in sequencing. From the Departament de Biologia Animal of Universitat de Barcelona, we would also like to thanks Dr. Miquel A. Arnedo and Elisa Mora de Checa for their help and advices on phylogenetic analyses and Dr. Juli Pujade-Villar for his comments on taxonomy issues. Thanks to Acciona Agua (Spain) for facilitate us the biological samples. Finally, our sincere thanks to Gusztav Hajnal and Akos Hajnal for translating the Hungarian language to the English.

REFERENCES

Altschul S. F., Gish W., Miller W., Myers E. W., Lipman D. J. (1990) Basic local alignment search tool. *J. Mol. Biol*. **215:** 403–410

Berger H., Foissner W. (2003) Biologische methoden der Gewässeranalysen: Ciliaten III-2.1. Illustrated guide and ecological notes to ciliate indicator species (Protozoa, Ciliophora) in running waters, lakes, and sewage plants. In: Steinberg, Calmano, Klapper, Wilken (Hrsg.): Handbuch angewandte Limnologie, **17**. Erg. Lfg. 1–160

Canals O., Salvadó H., Auset M., Hernández C., Malfeito J. J. (2013) Microfauna communities as performance indicators for an A/O Shortcut Biological Nitrogen Removal moving-bed biofilm reactor. *Water Res*. **47:** 3141–3150

Curds C. R. (1969) An illustrated key to the British Freshwater Ciliated Protozoa commonly found in activated sludge. London Her Majesty's Stationery Office; 54–55

Curds C. R. (1982) The ecology and role of protozoa in aerobic sewage treatment processes. *Ann. Rev. Microbiol*. **36:** 27–46

Elwood H. J., Olsen G. J., Sogin M. L. (1985) The small-subunit ribosomal RNA gene sequences from the hypotrichous ciliates *Oxytricha nova* and *Stylonychia pustulata*. *Mol. Biol. Evol*. **2:** 399–410

Fernández-Galiano D. (1994) The ammoniacal silver carbonate method as a general procedure in the study of protozoa from sewage (and other) waters. *Water Res*. **28:** 495–496

Foissner W., Berger H., Kohmann F. (1992) Taxonomische und ökologische Revision der Ciliaten des Saprobiensystems. In: Peritrichia, Heterotrichida, Odontostomatida, Band II. Bayerisches Landesamt für Wasserwirtschaft, München, 182–224

Foissner W., Berger H., Schaumburg J. (1999) Identification and ecology of limnetic plankton ciliates. Bayerisches Landesamt für Wasserwirtschaft, Deggendorf, Germany, 527–534

Giovannoni S. J., Delong E. F., Olsen G. J., Pace N. R. (1988) Phylogenetic Group-Specific Oligodeoxynucleotide Probes for Identification of Single Microbial Cells. *J. Bacteriol*. **170:** 720–726

Goloboff P. A., Farris J. S., Nixon K. C. (2008) TNT, a free program for phylogenetic analysis. *Cladistics* **24:** 774–786

Katoh K., Toh H. (2008) Recent developments in the MAFFT multiple sequence alignment program. *Brief. Bioinform*. **9:** 286–298. Available at http://mafft.cbrc.jp/alignment/server

Klein B. M. (1958) The 'dry' silver method and its proper use. *J. Protozool*. 5**:** 99–103

Lanfear R., Calcott B., Ho S. Y. W., Guindon S. (2012). PartitionFinder: combined selection of partitioning schemes and substitution models for phylogenetic analyses. *Mol. Biol. Evol*. **29:** 1695–1701

Littlewood D. T. J., Olson P. D. (2001) SSU rDNA and the Platyhelminthes: signal, noise, conflict and compromise. In: Interrelationships of the Platyhelminthes, (Eds. D. T. J. Littlewood, R. A. Bray) Taylor & Francis, London, 262–278

Medlin L., Elwood H. J., Stickel S., Sogin M. L. (1988) The characterization of enzymatically amplified eukaryotic l6S-like rRNA-coding regions. *Gene* **71:** 491–499

Müller K. (2005) SeqState: primer design and sequence statistics for phylogenetic DNA datasets. *Appl. Bioinform*. **4:** 65–69

Nenninger U. (1948) Die Peritrichen der Umgebung von Erlangen mit besonderer Berücksichtigung ihrer Wirtsspezifität. *Zool. Jb. Syst*. **77:** 169–266

Ronquist F., Huelsenbeck J. (2003) MrBayes 3: Bayesian phylogenetic inference under mixed models. *Bioinformatics* **19:** 1572–1574

Salvadó H., Gracia M. P., Amigó J. M. (1995) Capability of ciliated protozoa as indicators of effluent quality in activated sludge plants. *Water Res*. **29:** 1041–1050

Silvestro D., Michalak I. (2012) raxmlGUI: a graphical front-end for RAxML. *Org. Divers. Evol.* **12:** 335–337

Simmons M. P., Ochoterena H. (2000) Gaps as characters in sequence-based phylogenetic analyses. Syst. Biol. **49:** 369–381

Stamatakis A. (2014) RAxML Version 8: A tool for Phylogenetic Analysis and Post-Analysis of Large Phylogenies. *Bioinformatics* **30:** 1312–1313

Stiller J. (1971) Szájkoszorús Csillósok – Peritricha. Akadémiai Kiadó, Budapest, 23–73

Received on 9th February, 2015; revised on 17th April, 2015; accepted on 12th May, 2015